Assessing life-cycle seismic fragility of corroding reinforced concrete bridges through dynamic Bayesian networks

Molaioni, F.; Rinaldi, Z.; Andriotis, C.P.

DOI
10.1201/9781003323020-62

Publication date
2023

Document Version
Final published version

Published in
Life-Cycle of Structures and Infrastructure Systems

Life-Cycle of Structures and Infrastructure Systems – Biondini & Frangopol (Eds)

Assessing life-cycle seismic fragility of corroding reinforced concrete bridges through dynamic Bayesian networks

F. Molaioni & Z. Rinaldi
Department of Civil Engineering and Computer Science Engineering, University of Rome Tor Vergata, Rome, Italy

C.P. Andriotis
Faculty of Architecture and the Built Environment, Delft University of Technology, Delft, The Netherlands

ABSTRACT: Bridge structures are exposed to several chronic and abrupt stressors, among which the combined effects of corrosion and earthquakes pose a major threat to their long-term safety. Probabilistic risk assessment frameworks that quantify and propagate uncertainties inherent to these phenomena are necessary to mitigate this threat. This paper proposes a dynamic Bayesian network for state-dependent seismic fragility functions, capturing corrosion and seismic effects over time. Markovian transitions among deterioration states for different bridge components are developed, combining chloride diffusion and corrosion propagation models with non-stationary Gamma processes. State-dependent fragility curves are derived based on non-linear dynamic time-history analyses given possible degradation configurations of the structure, accounting for uncertainties in material, geometry, and deterioration parameters. Record-to-record variability is captured using synthetic ground motions. Results on a 4-span Gerber bridge showcase the suitability of the framework for describing life-cycle fragility, and its capacity for embedding in advanced algorithmic decision-making workflows is discussed.

1 INTRODUCTION

Bridges are infrastructure constituents of key socioeconomic importance, supporting vital road, rail, and pedestrian transportation systems. During their life-time, these structures must endure several continuous and sudden exogenous stressors.

Depending on the construction materials and environmental exposure, deterioration phenomena, such as corrosion, can have severe safety-reducing effects that increase over time (Vu & Stewart 1998). These become particularly critical when combined with extreme event hazards, such as those manifested in seismic-prone regions (Choe et al. 2008, Cui et al. 2018, Ghosh & Padgett 2010, Shekhar & Ghosh 2021).

Over the past century, the bridge construction sector has greatly focused on reinforced concrete designs due to material availability, cost-effectiveness, and structural performance considerations. A major deterioration factor for these structures, many of which are currently approaching or have well exceeded their design life, is corrosion of steel rebars (Bertolini et al. 2005), which exacerbates typical structural weaknesses against seismic loads. Besides strength and ductility reduction for the main concrete members due to rebar mass losses, corrosion also affects the performance of smaller, yet critical, bridge compartments, such as steel bearings, e.g. through plate thickness reduction, interlocking of sliding surfaces, and bolt failures (Mander et al. 1996). As such, bridges are heterogeneous time-dependent systems, where local component dynamics interact to eventually define global systemic behaviors and risks over the entire life-cycle. Numerous studies have dealt with the quantification of seismic safety losses deteriorating reinforced concrete bridges (Choe et al. 2008, Cui et al. 2018), also explicitly considering their multi-component character (Ghosh & Padgett 2010, Shekhar & Ghosh 2021).

Properly assessing structural safety losses is prerequisite for our ability to efficiently maintain the massive stock of aging concrete bridges, which is, in turn, paramount both for

DOI: 10.1201/9781003323020-62

minimizing the use of concrete in construction, thus curbing its major environmental impact, and for streamlining the immense economic needs of structural interventions. In that sense, managing structural integrity of existing bridges, requires not only at modeling of the aforementioned mechanical deterioration phenomena and their uncertainties, but also making these integrable with decision analysis frameworks.

In past years, the field of decision-making under uncertainties for existing structures has focused on coupling stochastic deterioration models, Bayesian decision principles, and advanced algorithmic procedures. Given the complexity of inspection and maintenance planning, featuring numerous possible actions in highly probabilistic environments, the problem has been shown to be efficiently defined within the global optimization framework of partially observable Markov decision processes (Andriotis & Papakonstantinou 2019, Morato et al. 2022). At the core of this formulation is expressing the deteriorating environment as a Dynamic Bayesian Network (DBN), which allows for efficient uncertainty propagation and inference over multiple time steps.

To address this need, this paper proposes a DBN approach allowing for updatable state-dependent seismic fragility functions, capturing long-term corrosion and seismic effects over time. The framework is applied to a case study bridge, modeled as a multi-component system, whose components are columns (COL), high type fixed bearings (HTFB), high type expansion bearings (HTEB), and low type fixed bearings (LTFB). In Section 2, the entire approach is described. First, the DBN structure is presented as well as the states which characterize it, namely the Corrosion Deterioration States (CDSs) and Seismic Damage States (SDSs). Then, the methodologies for determining both the conditional probabilities for Markovian transition among different corrosion damage states and the state-dependent seismic fragility curves are described. Section 3 is devoted to the case study bridge description to which the approach is applied. Then, in Section 4, the chloride corrosion probabilities over the lifetime of the structure are quantified and presented, as well as the state-dependent fragility curves, and the longitudinal effects of corrosion on the seismic fragility of column components. Finally, in Section 5, the main findings are summarized, underlining the suitability of the framework for capturing life-cycle fragility, as well as for being integrated with algorithmic decision-making workflows towards enhanced structural safety.

2 METHODOLOGY

2.1 *DBN for life-cycle seismic fragility of deteriorating bridges*

Seismic fragility functions represent the probability of a structure exceeding a seismic damage state (SDS), which quantifies structural damage in a discrete space in terms of an Engineering Demand Parameter (EDP), given an intensity measure (IM) of seismic action. As discussed in the previous section, seismic fragility is expected to increase over time due to structural deterioration for aging bridges. Therefore, encoding the corrosion intensity in a discrete space through the vector of corrosion deterioration state (CDS) of the system components, and the structural damage of those through the vector of seismic damage state (SDS), this probability can be expressed as:

$$\mathrm{P}_{SDS,t} = \mathrm{P}(\mathrm{SDS}_t \geq s | \mathrm{IM}_{0:t}, \mathrm{CDS}_{0:t}, \mathrm{SDS}_{0:t-1}) \tag{1}$$

where, without loss of generality, IM can also refer to vectors.

In this study, as an IM, the Peak Ground Acceleration (PGA) of the ground motion is used. For CDSs, rebars/bolts mass loss, $\mathrm{M}_{\mathrm{loss}}$ [%], steel plates thickness reduction, PTR [mm], and the additive coefficient of friction $\mathrm{k}_{\mathrm{corr}}$ [-], accounting for the interlocking effects due corrosion for expansion bearings, are used. The discretization and value ranges of these quantities are given in Table 1 for each component type, i.e. the columns component ($\mathrm{CDS}_{\mathrm{COL}}$), and the bearings component ($\mathrm{CDS}_{\mathrm{BEA}}$). SDSs for each component are defined trough lognormal distribution of EDPs according to (Ghosh & Padgett 2010), with respective thresholds shown in Table 2, for each component type. The inference of Eq. (1) requires, in general, the use of a large number of analyses, that must combine the effects of corrosion and seismic action over the structural lifetime. To solve this problem, a Dynamic Bayesian Network (DBN) for quantifying the risk of aging bridges over their life-cycle is here developed and shown in Figure 1. A DBN is a directed acyclic graphical model that is particularly suitable for modeling temporal patterns affected by uncertainties and can be used to easily solve inference problems. In such a model, variables are introduced through nodes, while conditional probabilities between these are represented by directed links. This way, it is possible to decompose the entire problem into smaller, easier-to-compute components by evaluating each probabilistic dependency with independent analyses.

The time-dependent nature of the seismic risk for aging structures is dynamically described through time-slices connected by conditional probabilities among CDS nodes, for which the Markovian assumption is considered. This way, CDS at time step t+1 depends only on the CDS in slice t:

$$P_{CDS,t} = P(CDS_0) \prod_{0}^{t-1} P(CDS_{\tau+1}|CDS_{\tau}) \tag{2}$$

To complete the description of the probabilistic graphical model, the following transitions between variables are introduced: the Markovian transition that describes the probability of having a corrosion state CDS=*j* at time t+1, given the corrosion state CDS=*i* at the previous time step t; and the state-dependent and time-invariant fragility functions, describing the probability of the bridge reaching a seismic damage state SDS, given the IM and the corrosion deterioration state CDS. It is worth noting that, as CDSs are discrete and the corrosion phenomenon is time-dependent, Markovian transitions are described by non-stationary matrices, while fragilities are continuous functions since the IM variable is not subject to discretization. In addition, Markovian transitions between SDS nodes over time may be introduced to consider that the resulting structural damage carries over to the next time step if no repair action is not taken.

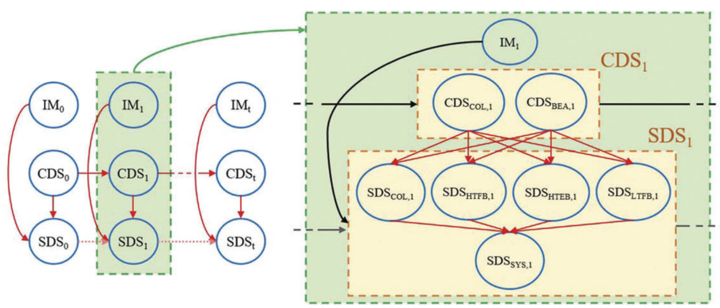

Figure 1. DBN for life-cycle seismic fragility of deteriorating bridges in this study. Overall model including nodes and transitions (left); Interactions of components and system states within the single time step (right).

Table 1. Corrosion Deterioration States.

CDS		0	1	2	3
Component	Parameter	LB-UB	LB-UB	LB-UB	LB-UB
Columns	M_{loss} [%]	0-0	0-15	15-30	30-45
Bearings	M_{loss} [%]	0-0	0-15	15-30	30-45
Bearings	PTR [mm]	0-0	0-3.5	3.5-5.1	5.1-6.5
Bearings	k_{corr} [-]	0-0	0-0.35	0.35-0.64	0.64-0.92

* M_{loss} = rebars/bolts mass lost, PTR = plates thickness reduction, k_{corr} = additive coefficient of friction for expansion bearings.

2.2 *Non-stationary transition for corrosion initiation and propagation*

Non-stationary transitions among CDSs are calculated through a probabilistic analytical assessment of the rebars/bolts mass loss, Mloss [%], over the life-time of the structure. The other corrosion parameters, i.e., PTR [mm] and k_{corr}, are assumed to follow the same transitions in accordance with the CDSs defined in Table 1. In addition, the transition for corrosion initiation and propagation are calculated separately to account for the two-phase nature of

Table 2. Probabilistic seismic damage states thresholds.

		Slight		Moderate		Extensive		Complete	
Component	EDP	M	D	M	D	M	D	M	D
COL	Curvature ductility [-]	1.29	0.59	2.1	0.51	3.52	0.64	5.24	0.65
HTEB-L	Displacement [mm]	37.4	0.6	104.2	0.55	136.1	0.59	187	0.65
HTEB-T, HTFB, LTFB	Displacement [mm]	6	0.25	20	0.25	40	0.47	187	0.65

* M = median of the lognormal distribution, D = Dispersion of the lognormal distribution, L = Longitudinal direction, T = Transverse direction.

the phenomenon. Chloride corrosion occurs when the chloride content at the depth of the bars, C, exceeds the critical threshold, C_{cr}, and thus destroys the protective film of the reinforcing bars, exposing them to aggressive agents. Chloride penetration into the concrete volume is captured by Fick's second law, under the assumption of constant chloride content at the outer surface (Choe et al. 2008, Cui et al. 2018, Ghosh and Padgett 2010, Shekhar & Ghosh 2021), C_s, and considering the diffusion coefficient, D_c, through the model proposed in (fib 2006). The time to corrosion initiation, T_{corr} [years], which defines the transition from CDS=0 to CDS=1, is thus determined by discretizing the structure life-time in yearly time-slices and determining the first slice when $C(x,t)>C_{cr}$.

Corrosion propagation over time is a phenomenon governed by environmental and concrete parameters and is strongly characterized by aleatoric uncertainties. To capture its randomness, the phenomenon is modeled through a Gamma process, in which the mean annual increase in uniform bar penetration is calculated with the model proposed by (Vu & Stewart 1998) and considering a CoV of 0.5 (fib 2006). To calculate the mass loss for steel rebars/bolts, which defines the CDS, a corrosion morphology model must be introduced. In this study, the model proposed by (Val & Melchers 1997), which relates the maximum penetration in the rebar with the mass lost through the pitting factor R (i.e., ratio between maximum and uniform penetration) is adopted. Furthermore, the pitting factor is considered as a random variable to account for the randomness of the corrosion morphology, following the probability distribution suggested in (Stewart & Al-Harthy 2008). The corrosion initiation time, T_{corr} [years], is also required in the propagation model, thus, the statistics obtained through the initiation model are used to consider its variability. Therefore, changes in CDSs are evaluated for each time step, *t*, by calculating the annual increase in rebar/bolt mass losses.

Non-stationary transitions for both the initiation and propagation phases represents the conditional probability of having CDS=*j* at time t+1, given that CDS=*i* at time-slice t. This probability is estimated as:

$$P(CDS_{t+1} = j | CDS_t = i) = \frac{\#(CDS_{t+1} = j \bigcap CDS_t = i)}{\#(CDS_t = i)} \tag{3}$$

For this study a sample size of 10^6 Monte Carlo simulations has been observed to be sufficient. More details on statistical properties adopted in this study for the random variables are given in Section 3.

2.3 *State-dependent fragility curves*

The state-dependent and time-invariant fragility functions are estimated by comparing probabilistic demand parameters and capacity limit states for structural components. Demand parameters for structural components, are determined using nonlinear dynamic analysis, and a suite of synthetic ground motions to account for the record-to-record variability (Vlachos et al. 2018). To account for uncertainties in materials, construction details, model, and seismic demand, 25 nominally identical but statistically different Finite Element (FE) models of bridges were considered, for which 250 synthetic ground motions were applied, resulting in a sample size of 6250 demand parameters. Three-dimensional FE models were set up using OpenSees (McKenna 2011). The non-linear behavior of structural components is taken into account for those considered as most vulnerable with respect to seismic and deterioration phenomena, i.e., COL, HTFB, HTEB, LTFB. For each structural component, 50 capacity values were sampled as per Table 2, and compared with the 6250 demand parameters, resulting in a total of 312500 SDS labels for component as a function of the IM.

This dataset was used for multinomial logistic regression, thus allowing the prediction of the probability of belonging to a given SDS as a function of IM through the softmax function (Andriotis et al. 2018). Therefore, the fragility for a limit state SDS=*i* is obtained through sum of the softmax functions related to the SDSs ≥ *i*:

$$\mathrm{P}(SDS_t \geq i|\mathrm{IM},\mathrm{CDS}) = \frac{\sum_{\mathrm{j=i}}^{\mathrm{J}} \mathrm{e}^{\beta_{0,i}+\beta_{1,i}\ln(\mathrm{IM})}}{\sum_{0}^{\mathrm{J}} \mathrm{e}^{\beta_{0,i}+\beta_{1,i}\ln(\mathrm{IM})}} \tag{4}$$

where J is the number of SDSs defined in Table 2, plus one, to consider the possibility of not activating any damage state. For the choice of multinomial logistic regression compared to other methodologies to define fragility functions the interested reader is referred to (Yi et al. 2022).

2.4 *Corrosion modeling of structural components*

The non-linear behavior of columns due to steel reinforcement corrosion has been considered by reducing as a function of M_{loss} the (i) reinforcement strength; (ii) concrete cover strength and stiffness; and (iii) concrete core confinement. Steel rebar and bolt yielding strengths have been reduced according to the degradation law for uniform and pitting corroded rebars proposed in (Imperatore et al. 2017). Note that the morphological nature of the corrosion is taken into account by considering uniform corrosion law if pitting factor R is lower than 4, and pitting corrosion law if R is higher than 4, thus identifying the type of corrosion as suggested in (Bertolini et al. 2005).

Concrete cover cracking following the expansion of the oxides produced by the corrosion process is accounted as proposed in (Coronelli & Gambarova 2004), and evaluating the average crack opening due to corrosion oxides expansion with the model proposed by (Vidal et al. 2004). In (Coronelli & Gambarova 2004), it is also suggested to consider the concrete cover stiffness reduction, which is accounted in this work in a simplified but safety-aware way, by neglecting the presence of the concrete cover upon exceedance of an average crack width of 1mm. Confinement losses of the concrete core, evaluated as proposed in (Mander et al. 1988), are accounted reducing the yielding strength of the stirrups. Bearings modeling approaches are based on the extensive study by (Mander et al. 1996), in which the experimental behavior of several types of steel bearings is compared with analytical methods, and in which valuable suggestions for the finite element modeling are reported. Following this approach, the mechanical behavior of these components is studied and modeled separately, with regard to the longitudinal and transverse direction of the bridge. For these components, the failure modes considered, as well as the analytical approaches for estimating the ultimate strength, even in the presence of corrosion, are referred to (Mander et al. 1996, Shekhar & Ghosh 2021).

3 CASE STUDY BRIDGE

The methodology described in the previous section is applied to an archetype 4-span bridge, representative of a wide range of seismic-vulnerable and deterioration-sensitive existing reinforced concrete bridges, present in infrastructure networks. The main geometrical features and finite element modeling choices are summarized in Figure 2. The deck has six prestressed I-beams, 1.5 m high, and presents two Gerber spans between half-joints. The column piers have a double circular cross-section of 1.3m diameter. Seismically vulnerable features of the bridge include the poor detailing of the columns as longitudinal reinforcement ratio equals 1% and circular stirrup spacing of 250mm, without any additional confinement in the dissipative zone.

For columns, nonlinear beam-column elements are used with appropriate (un)confined concrete and steel properties in OpenSees. The structural component is discretized along the height into three distinct elements. This way, since wide value ranges for CDSs are considered,

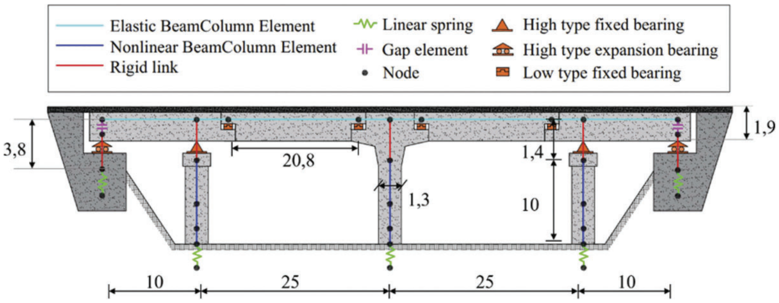

Figure 2. The studied 4-span Gerber bridge with respective geometrical and FE modeling features.

as shown in Table 1, the chance to have different corrosion intensity (M_{loss}) within the same CDS along the height of the column is accounted, thus the possibility of plastic hinges in zones away from the column base due to corrosion is captured (Yuan et al. 2017). The behavior of the bearings is modeled through friction and hysteretic links in the direction where displacements are constrained, and friction links only in the longitudinal direction for HTEB. Pile foundations are modeled using soil-foundation springs with linear behavior, abutments are modeled with linear translational springs, considering both passive and active stiffnesses. Abutment-deck gaps are modeled trough gap elements.

Following the definitions of (Duracrete 2000), environmental effects of both "splash" zone, representative of the use of de-icing salts, and "atmospheric zone" were compared. Moreover, "humid" exposure is considered. For the evaluation of CDSs transitions, the following random variables are assumed for components' materials and geometry: a lognormal distribution with mean 30 mm and CoV of 20% for the concrete cover depth; a discrete uniform distribution between [0.4,0.45,0.50] for the water-cement ratio; a normal distribution with mean 293° K and CoV of 2% for the actual temperature; and a Gumbel distribution with characteristics defined in (Stewart & Al-Harthy 2008) for the pitting factor. In addition, the other random variables in the chloride propagation model are assumed according to the values suggested in (Duracrete 2000, fib 2006, Choe et al. 2008). For the bridge FE model, the following random variables are considered for material properties: a normal distribution with a mean 43 MPa and CoV of 20% for the concrete mean cylindrical compressive strength; a lognormal distribution with mean 520 MPa and CoV of 10% for the steel yielding strength. The other material properties such as ultimate strain for (un)confined concrete, and steel stifnesses, are adopted as suggested in (Cui et al. 2018). Regarding values for random variables related to others modeling parameters, reference is made to (Nielson & DesRoches 2007).

4 RESULTS

In this section, the built model is applied for assessing the state-dependent fragility of the studied bridge. In Figure 3, the CDS probabilities, P_{CDS}, for structural components over the structural lifetime, relatively to both "splash" and "atmospheric" zones, are shown; these are generated by multiplying the observed non-stationary transitions by Eq (2). As expected, a higher probability of corrosion activation and propagation for the "splash" zone is found, as it is representative of a more chloride-aggressive environment. Environmental effects resulted in the following CDS probabilities after 100 years for the "splash" zone: $P_{CDS=0}$ =0.0289, $P_{CDS=1}$=0.2342, $P_{CDS=2}$=0.2374, $P_{CDS=3}$=0.4995; and on the other hand, for the "atmospheric" zone, the following CDS probabilities, P_{CDS}, after 100 years are found: $P_{CDS=0}$ =0.9726, $P_{CDS=1}$=0.0124, $P_{CDS=2}$=0.0064, $P_{CDS=3}$=0.0085. The results of seismic nonlinear dynamic analyses for column components are presented with respect to 4 corrosion scenarios, i.e., DCS_{COL} = 0 & DCS_{BEA} = 0, DCS_{COL} = 1 & DCS_{BEA} = 0, DCS_{COL} = 2 & DCS_{BEA} = 0, DCS_{COL} = 3 & DCS_{BEA} = 0. In Figure 4 the respective state-dependent fragility curves for column components are reported, thus showing the corrosion effects on their seismic safety.

The longitudinal effects of columns corrosion for their fragility for both "splash" and "atmospheric" are shown in Figure 5; these are obtained by combining the above results on non-stationary

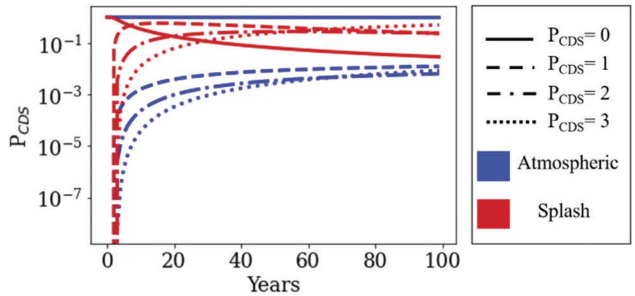

Figure 3. Probability for corrosion deterioration states (P_{CDS}) of structural components over their lifetime.

CDS probability and state-dependent fragilities through the weighted sum of the logistic functions based on P_{CDS}. This way, the suitability of the method for predicting time-varying fragility effects due to exposure to chloride-aggressive environments over the structural life is highlighted.

5 CONCLUSIONS

In this paper, a dynamic Bayesian network for life-cycle seismic fragility assessment of aging bridges is developed. The methodology is applied to a 4-span Gerber bridge case study, modeled as a multi-component structural system, with components referring to different columns and bearing types, to properly define seismic damage state characteristics under corrosion. Non-stationary Markovian transitions among deterioration states of the structural components are estimated through Monte Carlo simulation, and based on available probabilistic models for corrosion initiation and propagation. The seismic fragility with respect to five states of seismic damage is learned through multinomial logistic regression based on the results of nonlinear dynamic analyses, in which uncertainties in materials, geometry, modeling, seismic action and corrosion process are accounted. The results confirm the sensitivity of seismic responses to corrosion effects, and display how different aggressive environments can change the seismic safety of the bridge

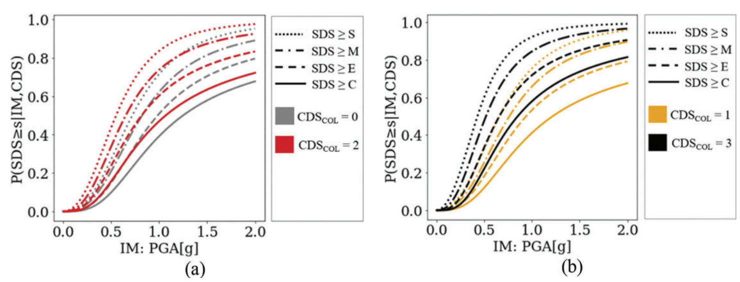

Figure 4. State-dependent fragility curves for the 4-span bridge columns. a) Comparison between scenarios CDS_{COL}= 0 and CDS_{COL}= 2; b) Comparison between scenarios CDS_{COL}= 1 and CDS_{COL}= 3.

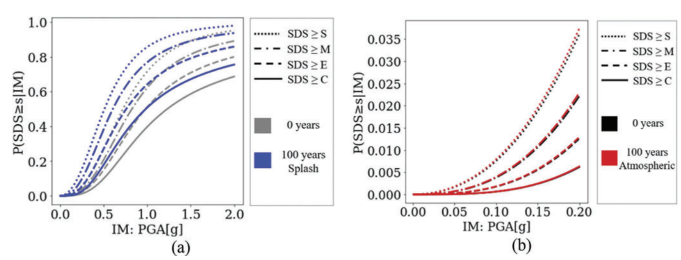

Figure 5. Time-varying effects on columns fragility for several chloride-aggressive environments. a) Effects after 100 years and "splash" zone; b) Effects after 100 years and "atmospheric" zone.

components over time. The proposed approach is an important step towards effective and flexible assessment and management of aging bridges structures. The DBN structure makes it possible to add new variables in the probabilistic graph without affecting those presented here, as well as to lend itself to advanced decision-support systems relying on Markov processes which can be consistently to the derived transition probabilities. Along these lines, possible extensions include, among others, consideration of residual structural capacity in the damage state definition, coupling of component limit states with non-seismic loads, and incorporation of action and observation variables for fragility updates based on inspection and maintenance outcomes.

REFERENCES

Andriotis, C. P., & Papakonstantinou, K. G. (2018). Extended and generalized fragility functions. *Journal of Engineering Mechanics*, *144(9)*, 04018087.

Andriotis, C. P., & Papakonstantinou, K. G. (2019). Managing engineering systems with large state and action spaces through deep reinforcement learning. *Reliability Engineering & System Safety, 191,* 106483.

Bertolini, L., Elsener, B., Pedeferri, P., & Polder, R. (2005). Corrosion of Steel in Concrete: Prevention, Diagnosis, Repair.

Choe, D. E., Gardoni, P., Rosowsky, D., & Haukaas, T. (2008). Probabilistic capacity models and seismic fragility estimates for RC columns subject to corrosion. *Reliability Engineering and System Safety*, *93(3)*, 383–393.

Coronelli, D., & Gambarova, P. (2004). Structural assessment of corroded reinforced concrete beams: Modeling guidelines. *Journal of Structural Engineering*, *130(8)*, 1214–1224.

Cui, F., Zhang, H., Ghosh, M., & Xu, Y. (2018). Seismic fragility analysis of deteriorating RC bridge substructures subject to marine chloride-induced corrosion. *Engineering Structures, 155,* 61–72.

Duracrete. 2000. Probabilistic performance based durability design of concrete structures. Final Technical Rep. (Document BE95-1347/R17). Lyngby, Denmark: European Union—Brite EuRam III

Ghosh, J., & Padgett, J. E. (2010). Aging considerations in the development of time-dependent seismic fragility curves. *Journal of Structural Engineering*, *136*(12), 1497–1511.

Imperatore, S., Rinaldi, Z., & Drago, C. (2017). Degradation relationships for the mechanical properties of corroded steel rebars. *Construction and Building Materials, 148, 219–230*.

fib, F. I. B. (2006). Model code for service life design. Model code.

Mander, J. B., Priestley, M. J., & Park, R. (1988). Theoretical stress-strain model for confined concrete. *Journal of structural engineering*, *114(8)*, 1804-1826.

Mander, J. B., Kim, D.-K., Chen, S. S., & Premus, G. J. (1996). Response of Steel Bridge Bearings to Reversed Cyclic Loading.

McKenna, F. (2011). OpenSees: A framework for earthquake engineering simulation. *Computing in Science and Engineering*, *13(4)*, 58–66.

Morato, P. G., Andriotis, C. P., Papakonstantinou, K. G., & Rigo, P. (2022). Inference and dynamic decision-making for deteriorating systems with probabilistic dependencies through Bayesian networks and deep reinforcement learning.

Nielson, B. G., & DesRoches, R. (2007). Seismic fragility methodology for highway bridges using a component level approach. *Earthquake Engineering and Structural Dynamics*, *36(6)*, 823–839.

Shekhar, S., & Ghosh, J. (2021). Improved Component-Level Deterioration Modeling and Capacity Estimation for Seismic Fragility Assessment of Highway Bridges. *ASCE-ASME Journal of Risk and Uncertainty in Engineering Systems, Part A: Civil Engineering*, *7(4)*.

Stewart, M. G., & Al-Harthy, A. (2008). Pitting corrosion and structural reliability of corroding RC structures: Experimental data and probabilistic analysis. *Reliability Engineering and System Safety*, *93(3)*, 373–382.

Val, D.V. and Melchers, R. E. (1997). Reliability of Deteriorating RC Slab Bridges. *Journal of Structural Engineering,* 1638–1644.

Vidal, T., Castel, A., & François, R. (2004). Analyzing crack width to predict corrosion in reinforced concrete. *Cement and Concrete Research*, *34(1)*, 165–174.

Vlachos, C., Papakonstantinou, K. G., & Deodatis, G. (2018). Predictive model for site specific simulation of ground motions based on earthquake scenarios. *Earthquake Engineering and Structural Dynamics*, *47(1)*, 195–218.

Vu, K. A. T., & Stewart, M. G. (2000). Structural reliability of concrete bridges including improved chloride-induced corrosion models. *Structural Safety*.

Yi, S., Papakonstantinou, K. G., Andriotis, C. P., & Song, J. (2022). Appraisal and mathematical properties of fragility analysis methods. In *Proceedings of the 13th International Conference on Structural Safety and Reliability (ICOSSAR)*.

Yuan, W., Guo, A., & Li, H. (2017). Seismic failure mode of coastal bridge piers considering the effects of corrosion-induced damage. *Soil Dynamics and Earthquake Engineering*.